

## 1s-2p Transitions in Mg Bombarded with 21-MeV Oxygen Ions<sup>†</sup>

D. G. McCrary,\* M. Senglaub, and Patrick Richard

*The University of Texas, Austin, Texas 78712*

(Received 3 December 1971)

A thick Mg target was bombarded by a 21-MeV oxygen-ion beam. Nine 1s-2p transitions were observed with an energy resolution of 1.26 eV. Relative to the 1253.6-eV  $K\alpha_{1,2}$  reference energy, the energies of the other observed transitions in units of eV were 1261.5, 1268.5, 1270.7, 1273.3, 1281.0, 1283.0, 1293.0, and 1295.4. By comparing with Hartree-Fock-Slater calculations, the five groups of peaks were found to correspond to 1s-2p ( $K\alpha$ ) transitions with initial configurations  $(1s)^{-1}(2p)^{-n}$  for  $n=0, 1, 2, 3,$  and 4. The transition for the  $(1s)^{-1}(2p)^{-5}$  initial configuration was not observed in this experiment. This can be attributed to self-absorption in the target since the  $(1s)^{-1}(2p)^{-5}$   $K\alpha$  transition energy lies above the  $K$  absorption edge.

### I. INTRODUCTION

The observation of a shift to higher energies of characteristic x-rays produced by heavy-ion bombardment has created renewed interest in the x-ray production mechanism and heavy-ion-atom interaction processes.<sup>1-6</sup> To aid in the understanding of these processes, several experiments with high-resolution spectrometers have recently been conducted.<sup>7-9</sup> Knudson *et al.*,<sup>7</sup> using a 5-MeV  $N^+$ -ion beam to bombard an Al target, were able to resolve the  $K\alpha$  x-ray transition into six components. From Hartree-Fock-Slater (HFS) calculations these lines were attributed to the deexcitation of atoms with initial hole configurations  $1s^{-1}2p^{-n}$ , where  $n=0, 1, 2, 3, 4,$  and 5. In a similar experiment<sup>8</sup> with an oxygen beam bombarding an Fe target, the  $K\alpha$  spectrum was resolved into three lines arising from the deexcitation of atoms with initial hole configurations of  $1s^{-1}2p^{-n}$ , where  $n=0, 1,$  and 2. In a third experiment,<sup>9</sup> a crystal spectrometer was used to analyze the  $K$  x rays produced by a 30-MeV oxygen beam on a Si target. Six component groups corresponding to atoms with initial hole configurations of  $1s^{-1}2p^{-n}$ , where  $n=0, 1, 2, 3, 4,$  and 5, were seen. Three of the groups were resolved doublets.

In the present experiment, a 21-MeV  $O^{5+}$  beam was used to bombard a thick Mg target. The x rays were analyzed with a high-resolution Bragg-Soller crystal spectrometer. In this case, five component groups were resolved corresponding to deexcitation of atoms with initial hole configurations of  $1s^{-1}2p^{-n}$ , where  $n=0, 1, 2, 3,$  and 4. Two of the groups were resolved doublets and a third one a resolved triplet. It is thought that the line corresponding to the deexcitation of the atom with initial hole configuration  $1s^{-1}2p^{-5}$  was not seen because of self-absorption in the target since its energy lies just above the  $K$  absorption edge of Mg. The energy resolution realized was 1.26 eV.

### II. EXPERIMENTAL SETUP

The data for this paper were taken with a Bragg-Soller crystal spectrometer.<sup>10</sup> The essential features of the vacuum spectrometer are depicted in Fig. 1. They include an entrance Soller collimator that can be adjusted by a spring-loaded micrometer, a table on which the crystal is positioned, and a larger table to which the vertical exit Soller slits and detector are attached. The front Soller slits have an angular divergence of 2 min. The exit slits have an angular divergence of 20 min. Two high-precision milling tables in a vertical arrangement turn the detector and crystal tables. The detector table rests on the upper milling table and can be turned independently of the crystal table which is connected by a shaft to the lower milling table. When data are taken, the spectrometer is attached at 90° to a target chamber by bellows. The Soller slit housings are also attached with bellows to two of seven ports on the vacuum chamber which houses the crystal. The ports to which the Soller slit housings are attached are chosen so that the  $2\theta$  angle of the detector is within the limits of the extended bellows connecting the Soller slit and crystal housing.

A flow proportional counter was mounted behind the exit Soller slits. A 2- $\mu$  Hostophan<sup>11</sup> window set the efficiency of the counter between 70 and 75% over the energy range 1250-1300 eV.

An ammonium-dihydrogen-phosphate (ADP) crystal ( $2d=10.642 \text{ \AA}$ ) was used to analyze the x rays. Figure 2 gives a plot of x-ray energy in keV and  $\Delta E$  in eV versus the Bragg angle ( $\theta_B$ ) in degrees for an ADP crystal. The solid curve in the figure refers to the x-ray energy, and the dashed curve refers to the resolution  $\Delta E$ . For an ADP crystal with  $2d=10.642 \text{ \AA}$ , the calculated resolution for the Mg  $K\alpha_{1,2}$  transition is 0.4 eV. The measured full width at half-maximum, however, of the Mg  $K\alpha_{1,2}$  transition was found to be 1.26 eV. The

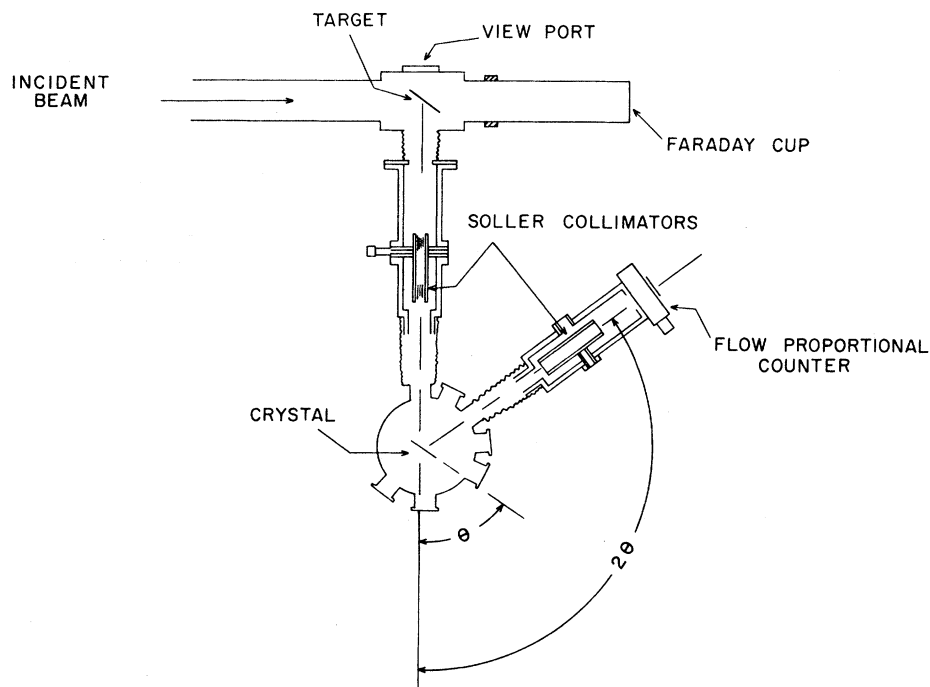


FIG. 1. Schematic of Bragg-Soller crystal spectrometer attached to the tandem Van de Graaff beam line.

observed energy resolution comes from two main sources: (i) collimation and (ii) crystal imperfections or crystal rocking curve. Adding the two contributions in quadrature yields a crystal rocking curve of 6 arcmin, which in the present case adds 1.2-eV broadening to the x-ray peaks.

The Mg target was cut from a thick Mg metal sheet which stopped the beam completely and was positioned at a  $45^\circ$  angle to the incident beam.

Figure 3 is a schematic of the electronic setup of the system. The system can be operated in any of three modes. In the first mode, data are taken manually. The experimenter rotates the spectrometer turntables by means of the motor control unit which steps the motors. He then records the number of counts/ $\mu\text{C}$  at each position. In the second mode the experimenter steps the spectrometer and starts the scaler manually, however, a PDP-7 computer accumulates the counts/ $\mu\text{C}$  at each point and histograms the results. The third mode of operation is completely computer controlled. At each datum point the computer records the number of counts for a preset number of  $\mu\text{C}$ , and steps the crystal and detector a predefined angular distance. After a 1-sec pause following the stepping operation, the computer begins accumulating detector and integrator pulses for the new angular setting. The data for this experiment were taken in the first mode.

The detector high-voltage power supply was set at +2000 V. Pulses from the detector were sent through a preamp and amplifier. From the prompt

output of the amplifier, the pulses were sent to a single-channel analyzer (SCA) and then to a slave

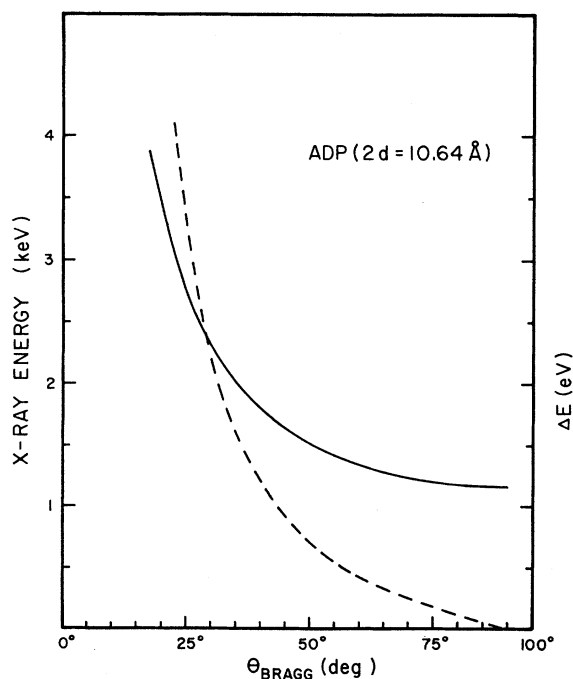


FIG. 2. A plot of x-ray energy in keV and  $\Delta E$  in eV vs  $\theta_B$  in degrees for an ADP crystal ( $2d = 10.64 \text{ \AA}$ ). One division equals 1 eV for  $\Delta E$ . The solid curve refers to the x-ray energy and the dashed curve refers to the resolution.

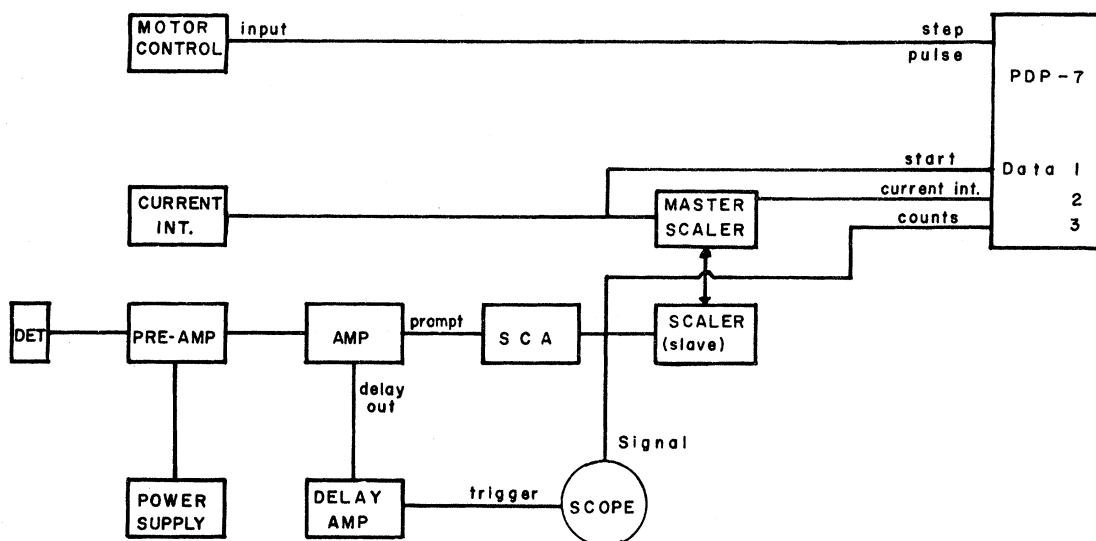


FIG. 3. Block diagram of electronics.

scaler. The window of the SCA was set using the delayed output of the amplifier to trigger an oscilloscope which monitored the output of the SCA. The slave scaler was controlled by a master scaler that counted the pulses from the current integrator.

### III. RESULTS AND DISCUSSION

The Mg  $K\alpha$  spectrum taken in this experiment can be seen in Fig. 4. This spectrum is very similar

to the Si and Al  $K\alpha$  spectra<sup>7,9</sup> mentioned previously. An obvious deviation of the Mg spectrum from the first two is the absence of the line of highest energy. This line corresponds to the Si and Al lines that are formed from the deexcitation of an atom with an initial hole configuration of  $1s^{-1}2p^{-5}$ . The HFS calculated energy for this line in Mg is 1313 eV. If this number is correct, then the intensity of the line should be weakened because of self-absorption

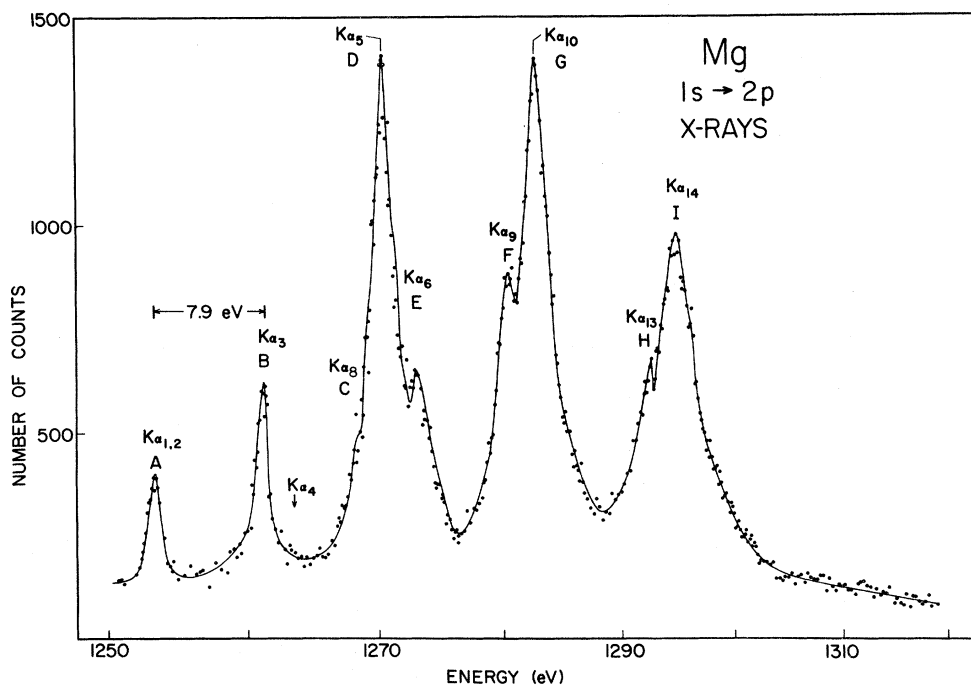


FIG. 4. Mg  $K\alpha$  satellite lines produced by 21-MeV oxygen bombardment. The number of counts represents the yield for a given number of  $\mu\text{C}$  of beam on the target.

TABLE I. Mg  $K\alpha$  lines from 21-MeV oxygen bombardment.

Label <sup>a</sup>	Relative intensity	$\theta_B$	Energy (eV) <sup>b</sup>
A	1.0	68° 19' 38''	1253.6 <sup>c</sup>
B	2.13	67° 26' 33''	1261.5
C		66° 41' 33''	1268.5
D	11.06	66° 27' 38''	1270.7
E		66° 11' 48''	1273.3
F		65° 25' 38''	1281.0
G	10.92	65° 13' 48''	1283.0
H		64° 17' 33''	1293.0
I	8.10	64° 4' 3''	1295.4

<sup>a</sup>Labels refer to peaks in Fig. 4.

<sup>b</sup>The uncertainty in peaks B, D, G, and I is  $\sim 0.4$  eV and in peaks C, E, F, and H it is  $\sim 0.6$  eV. At these angles the energy dispersion is 0.16 eV/arcmin, so that a 0.4-eV uncertainty corresponds to a 2.5-min uncertainty.

<sup>c</sup>Reference 12 value.

in the target, since the Mg  $K$  absorption edge is at 1305 eV.<sup>12</sup>

Table I contains the analyzed data from the Mg spectrum shown in Fig. 4. The second column contains the relative intensities of the five component groups normalized to the  $K\alpha_{1,2}$  peak. No correction was made for the variation of crystal reflectivity as a function of Bragg angle. The third column gives the observed crystal Bragg angle. The first value was calculated using the tabulated energy<sup>12</sup> of the  $K\alpha_{1,2}$  transition together with the measured  $2d$  spacing of this crystal.<sup>9</sup> The remainder are the values obtained from the spectrometer with a small zero-angle correction calculated from the measured  $K\alpha_{1,2}$  Bragg angle.<sup>9</sup> The fourth column gives the calculated energies in which, as mentioned above, the  $K\alpha_{1,2}$  energy is taken from Ref. 12.

The case of Mg  $K\alpha$  x-ray transitions has been studied in much detail by standard electron-bombardment and crystal-spectrometer techniques. One example of this is the work of Kunzl,<sup>13</sup> who observed many weak x-ray lines above the Mg  $K\alpha_{1,2}$  transition energy and classed these as Mg satellite lines. Table II compares our data to those of Kunzl. The third column gives our transition energy and the value Kunzl found in his work. Kunzl has identified a Mg line corresponding to each line seen in the present experiment. The fourth column gives the designation of the transitions as defined by Kunzl. The fifth column gives the energy difference between the satellite lines and the  $K\alpha_{1,2}$  line for the present data and for Kunzl's data. The sixth column contains the HFS calculated energies for the various initial hole configurations  $(1s)^{-1}(2p)^{-n}$ .

The satellite lines  $K\alpha_3$  and  $K\alpha_4$  separated by 2 eV are observed by Kunzl as the strongest satellite lines and occur with approximately the same intensity. For the heavy-ion bombardment the Mg  $K\alpha_3$  peak is observed, however, the  $K\alpha_4$  peak is not seen. For the case of the Si plus 30-MeV oxygen bombardment data of McCrary and Richard,<sup>9</sup> the  $K\alpha_3$  and  $K\alpha_4$  lines are both observed with the  $K\alpha_4$  peak being a very small shoulder on the larger  $K\alpha_3$  peak. These two satellite lines occur near the HFS energy for the transition  $(1s)^{-1}(2p)^{-1} \rightarrow (2p)^{-2}$ . The initial and final states can couple to several spins, thus giving rise to several possible  $E1$  transitions. The separation of these different lines is much smaller than the separation between the component groups  $(1s)^{-1}(2p)^{-n} \rightarrow (2p)^{-n-1}$  for  $n=0, 1, 2, 3, 4,$  and  $5$ . If the population of the various spin states were determined completely according to statistics, then the ratio of  $K\alpha_3$  to  $K\alpha_4$  would be independent of the type of particles inducing the inner-shell ionization. The various sets of data do not support this hypothesis.

The next most intense satellite lines observed by Kunzl are the  $K\alpha_5$  and  $K\alpha_6$  lines, which also have about equal intensity. In the heavy-ion excitation the Mg  $K\alpha_5$  and  $K\alpha_6$  lines are clearly resolved; however, the  $K\alpha_5$  line is much stronger than the  $K\alpha_6$  line. These two lines plus the  $K\alpha_8$  line make up part of the  $(1s)^{-1}(2p)^{-2} \rightarrow (2p)^{-3}$  x-ray multiplet.

The multiplet of states formed by the  $(1s)^{-1}(2p)^{-3} \rightarrow (2p)^{-4}$  transition has about the same intensity as the  $(1s)^{-1}(2p)^{-2} \rightarrow (2p)^{-3}$  multiplet discussed above. The shapes of the two multiplets are nearly mirror images of each other with the  $K\alpha_5$  peak approximately the same height as the  $K\alpha_{10}$  peak and the separation between  $K\alpha_9$  and  $K\alpha_{10}$  being 2.0 eV and between  $K\alpha_5$  and  $K\alpha_6$  being 2.6 eV. In the case of electron excitation, the Mg  $K\alpha_9$  and  $K\alpha_{10}$  satellites are extremely weak.

The comparison of the  $(1s)^{-1}(2p)^{-4} \rightarrow (2p)^{-5}$  transition multiplet observed here to the extremely weak  $K\alpha_{13}$  and  $K\alpha_{14}$  satellites reported by Kunzl is somewhat dubious, since the observed energies do not correspond very well and since the peaks assigned by Kunzl are in a region of his spectrum where there are many small fluctuations.

It should be pointed out that the intensity ratios shown by Kunzl are not very reliable, as they are taken from photographic plates. This may explain some of the discrepancies between his intensity ratios and the present results.

Table III gives a summary of the observed  $1s \rightarrow 2p$  transition energies of Si, Al, and Mg and their respective  $K$  absorption edges. From these data it can be seen that the transitions in Si and Al involving the initial hole configuration  $1s^{-1}2p^{-5}$  lie just below the absorption edges, whereas in Mg

TABLE II. Mg  $K\alpha$  lines from 21-MeV oxygen bombardment.

Label <sup>a</sup>	Relative intensity	Energy (eV)		Kunzl's designation <sup>b</sup>	$E - E_{\alpha_{1,2}}$ (eV)		HFS calculations	
		Present	Kunzl <sup>b</sup>		Present	Kunzl <sup>b</sup>	Energy (eV)	Initial config.
A	1.0	1253.6 <sup>c</sup>	1254	$K\alpha_{1,2}$	0	0	1254	$(1s)^{-1}$
...	...	...	1259	$K\alpha'$	...	5	...	...
B	2.13	1261.5	1262	$K\alpha_3$	7.9	8	1262	$(1s)^{-1}(2p)^{-1}$
...	...	...	1264	$K\alpha_4$	...	10		
C		1268.5	1269	$K\alpha_6$	14.9	15		
D	11.06	1270.7	1271	$K\alpha_5$	17.1	17	2172	$(1s)^{-1}(2p)^{-2}$
...	...	...	1272	$K\alpha_7$	...	18		
E		1273.3	1274	$K\alpha_8$	19.7	20		
F		1281.0	1278	$K\alpha_9$	27.4	24		
G	10.92	1283.0	1283	$K\alpha_{10}$	29.4	29	1284	$(1s)^{-1}(2p)^{-3}$
H		1293.0	1288	$K\alpha_{13}$	39.4	34		
I	8.10	1295.4	1291	$K\alpha_{14}$	41.8	37	1298	$(1s)^{-1}(2p)^{-4}$
...	...	...	...	...	...	...	1313	$(1s)^{-1}(2p)^{-5}$

<sup>a</sup>Labels refer to peaks in Fig. 4.<sup>b</sup>Taken from Ref. 13.<sup>c</sup>Reference 12 value.

the transition occurs above the absorption edge which supports the explanation given for not seeing the highest-energy line in Mg.

#### IV. CONCLUSION

This experiment further demonstrates the very dramatic departure of the atom-ion collision mechanism from the collision mechanism for incident electrons, photons, protons, or  $\alpha$  particles. The spectra given here imply a high probability for the production of multiple inner-shell ionization in the target atom as a result of a single collision with high-energy heavy ions in the 1-MeV/amu range as opposed to the predominant single  $K$ -shell ionization resulting from a single collision with incident electrons, photons, protons, or  $\alpha$  particles. The primary population of the various ionic species as a result of the collision is not determined from this experiment. What is observed is the  $K\alpha$  transition of an ionic state of the atom in which the  $K\alpha$  transition rate is comparable to other possible transition rates and can thus compete favorably. This ionic state is not necessarily formed directly as a result of the high-energy collision but rather may be reached through other transitions such as Coster-Kronig, Auger, etc., which still leave the atom with a  $(1s)$  hole. An argument which demonstrates that this can indeed happen is the following: One would expect from a statistical argument that there would be  $(2s)$  holes produced in the atom as well as  $(2p)$  holes. This would lead to seven rather than five  $K\alpha$  peaks above the  $K\alpha_{1,2}$  peak. However, the  $LLM$  transition rate far exceeds the  $K\alpha$  rate, so that  $(2s)$  holes are quickly transferred to  $(2p)$  holes in the atom.

Another important possibility which has not yet been established or eliminated is that of double  $K$ -shell ionization in the target atom-ion collision. This ionic state can possibly lead to various multiple  $L$ -shell vacancies prior to a  $K\alpha$  transition. The existence of this state can hopefully be found by means of a  $K$  x-ray,  $K$  x-ray coincidence experiment.

New important information about the reaction mechanism can be had by observing the Auger-electron spectra following atom-ion collisions. Much attention should be given to this problem. Auger-electron spectroscopy is a valuable complement to the x-ray data, since the Auger transitions are not restricted by the electromagnetic selection rules which x-ray transitions are bound to. In addition, many of the transitions which may compete

TABLE III. Observed  $1s \rightarrow 2p$  transition energies and absorption edges for Mg, Al, and Si.

Initial hole config.	Mg observed $E$ (eV)	Al observed <sup>a</sup> $E$ (eV)	Si observed <sup>b</sup> $E$ (eV)
$(1s)^{-1}$	1253.6 <sup>c</sup>	1486	1739.8
$(1s)^{-1}(2p)^{-1}$	1261.5	1496	1750.8
$(1s)^{-1}(2p)^{-2}$	1270.7	1507	1762.6
$(1s)^{-1}(2p)^{-3}$	1283.0	1521	1778.8
$(1s)^{-1}(2p)^{-4}$	1295.4	1534	1794.2
$(1s)^{-1}(2p)^{-5}$	...	1548	1809.7
Absorption energy	1305	1559	1838

<sup>a</sup>Taken from Ref. 7.<sup>b</sup>Taken from Ref. 9.<sup>c</sup>Reference 12 value.

with the  $K\alpha$  transition should be observable in the Auger spectrum.

The various atomic rearrangement processes which are probably occurring in the excited target ions as discussed above are evidently influenced by strong electron correlation effects. This is

suggested by the observation of similar  $K\alpha$  spectra for Mg plus 21-MeV oxygen (present work), Si plus 30-MeV oxygen,<sup>9</sup> Al plus 5-MeV nitrogen,<sup>7</sup> and Al plus 18-MeV oxygen.<sup>14</sup> That is, the relative intensities of the peaks appear to be nearly independent of bombarding energy above 5 MeV.

<sup>†</sup>Work supported in part by the Robert A. Welch Foundation and the U.S. AEC.

\*Present address: University of Texas Medical School, Dallas, Tex.

<sup>1</sup>P. Richard, I. L. Morgan, T. Furuta, and D. Burch, *Phys. Rev. Letters* **23**, 1009 (1969).

<sup>2</sup>D. Burch and P. Richard, *Phys. Rev. Letters* **25**, 983 (1970).

<sup>3</sup>P. H. Mokler, *Phys. Rev. Letters* **26**, 811 (1971); R. C. Der *et al.* (unpublished).

<sup>4</sup>G. A. Bissinger and S. M. Shafroth, *Bull. Am. Phys. Soc.* **16**, 125 (1971).

<sup>5</sup>H. J. Specht, *Z. Physik* **185**, 30 (1965).

<sup>6</sup>M. E. Cunningham *et al.*, *Phys. Rev. Letters* **24**,

931 (1970).

<sup>7</sup>A. R. Knudson, D. J. Nagel, P. G. Burkhalter, and K. T. Dunning, *Phys. Rev. Letters* **36**, 1149 (1971).

<sup>8</sup>D. Burch, P. Richard, and R. L. Blake, *Phys. Rev. Letters* **26**, 1355 (1971).

<sup>9</sup>D. G. McCrary and P. Richard, *Phys. Rev. A* (to be published).

<sup>10</sup>R. L. Blake, Ph.D. dissertation (University of Colorado, 1968) (unpublished).

<sup>11</sup>Siemens, Catalog No. C70144-A952-B40.

<sup>12</sup>J. A. Bearden, *Rev. Mod. Phys.* **39**, 78 (1967); J. A. Bearden and A. F. Burr, *ibid.* **39**, 125 (1967).

<sup>13</sup>V. Kunzl, *Z. Physik* **99**, 481 (1936).

<sup>14</sup>M. Senglaub *et al.* (unpublished).

## Coulomb $T$ Matrix and the Proton-Hydrogen Charge Exchange

C. S. Shastry, A. K. Rajagopal, and J. Callaway

*Department of Physics and Astronomy, Louisiana State University*

*Baton Rouge, Louisiana 70803*

(Received 3 September 1971; revised manuscript received 6 March 1972)

The proton-hydrogen charge-exchange amplitude is evaluated using the first-order terms in the Faddeev expansion for the corresponding transition operator. The new Coulomb  $T$  matrix derived by us recently is employed in computing the cross sections. For high energies of the incident proton, the Coulomb  $T$  matrix approaches the Coulomb potential to order  $v^{-1} \ln v$  in contrast to the situation for a short-range potential ( $\sim v^{-2}$ ). In the extreme high-energy limit the results of the first-order Faddeev-Watson approximation approach those of the Jackson-Schiff approximation. Explicit numerical calculation in the energy region 100 keV to 3 MeV shows that the cross sections lie in between those of the Brinkman-Kramers and Jackson-Schiff (JS) results and they approach the JS results from above. This is in contradistinction to our previous work based on an incorrect form of the  $T$  matrix.

### I. INTRODUCTION

Since the pioneering work of Faddeev<sup>1</sup> on three-particle scattering, there has been a revival of interest in the classical problems of the Coulomb  $T$  matrix<sup>2-8</sup> and the behavior of the proton-hydrogen charge-exchange amplitude.<sup>9-15</sup> Lively controversies exist in each case. This work concerns both problems and should reduce some of the confusion.

We begin with a brief survey of the relevant history. A more complete review of work prior to 1968 has been given by Bransden.<sup>16</sup> The high-energy limit of the proton-hydrogen charge exchange was first calculated by Brinkman and Kramers<sup>17</sup> (BK) who evaluated the transition amplitude in the first Born approximation but neglected the interaction between the protons. The neglect of this term

is made plausible by a physical argument based on the impact parameter approximation.

Jackson and Schiff<sup>18</sup> (JS), who were aware of the impact-parameter argument, found that the inclusion of the proton-proton interaction reduced the cross section in the high-energy limit by a factor of 0.66 compared to the BK result.

Subsequently, second-order terms in the Born series were calculated by Drisko<sup>19</sup> and third-order terms were estimated. The result is

$$\sigma = \sigma_{\text{BK}}(0.319 + 5\pi v/2^{12}),$$

where  $\sigma_{\text{BK}}$  is the Brinkman-Kramers cross section and  $v$  is the speed of the incident proton in a.u. in the laboratory system. This calculation indicated that no matter how high the energy, the Born series does not converge to its first term. Other calcula-